1, 79, 2367 (1983).
33. C. N. Egly and C. F. Wells, *J. Chem. Soc. Dalton*, 1617 (1982).
34. I. M. Sidahmed and C. F. Wells, *J. Chem. Soc. Dalton*, 1035 (1983).
35. G. Scatchard, *Chem. Rev.*, 44, 7 (1949).
36. F. Franks, "Hydrogen-bonded Solvent System", Eds. A. K. Covington and P. Jones, Taylor and Francis, London, p. 31 and pp. 211-219, 1968.

Computer Graphics / Molecular Mechanics Studies of Quinolones Geometry Comparison with X-ray Crystal Structures

Sung Kee Chung*

Department of Chemistry, Pohang Institute of Science and Technology, Pohang 790-600

Daniel F. Chodosh

Distributed Chemical Graphics, Inc. 1326 Carol Road, Meadowbrook, PA 19046, U.S.A.

Received March 12, 1990

Geometries for several representative quinolone carboxylate type antibaterials have been calculated by computer graphics/molecular mechanics energy minimization procedures using both MM2 and AMBER force fields. The calculated geometries were found to be in reasonable agreements with the corresponding X-ray crystal structures. It has been pointed out that notwithstanding the weaknesses associated with calculating the resonance and hydrogen bonding contributions, the employed methods are capable of generating credible ring geometries and torsional angle dispositions of N(1)-ethyl and 3-carboxylate substituents of the quinolones.

Introduction

During the last dacade or so, the 4-pyridone-3-carboxylate class of antibacterials, collectively known as quinolones, has been extensively explored in the pharmaceutical laboratories. Nalidixic acid, discovered more than 25 years ago as the first therapeutically useful quinolone, suffered from the lack of a substantial gram positive activity and the poor tissue distribution. In the early 1980's, significant improvements in potency and biospectrum were achieved with syntheses of 6-fluoro and 7-aminosubstituted derivatives, resulting in the development of currently marketed drugs such as norfloxacin, ciprofloxacin, pefloxacin, ofloxacin and enoxacin.[1]

Despite the clinical improtance, the bacteriocidal mode of action of these compounds is not well understood. It is generally accepted that quinolones inhibit DNA-synthesis by interfering with the ATP-dependent DNA-supercoiling process catalyzed by bacterial DNA-gyrase. Fairly extensive studies have been carried out on the correlation between the minimum inhibitory cconcentration(MIC) and the *in vitro* gyrase inhibition, as well as on the binding of quinolones to DNA-gyrase and various natural and synthetic pieces of DNA in attempts to understand the molecular mechanism of the inhibition.[2] It was initially supposed that the mechanism of action might involve a covalent interaction between a bio-nucleophile on the A-subunit of the enzyme and the β-amino-enone moiety of quinolones, and that the nucleophilic 1,4-addition process might also be facilitated by a metal complexation with the β-keto-carboxylate moiety of the quinolone structure.[3] However, the *in vitro* model experiments show that the quinolone ring system is not very susceptive to such a Michael attack by a number of organic nuclephiles.[4]

Very recently, Shen *et al.* have proposed a cooperative quinolone-DNA binding model for the inhibition of DNA-gyrase. According to this model, the initial binding of gyrase to the relaxed DNA substrate induces a specific quinolone binding site in the DNA in the presence of ATP. The binding affinity and specificity are derived from two key features, *i.e.*, the specific conformation of the proposed single-stranded DNA pocket induced by the enzyme and the unique self-association of the quinolone molecules to fit the binding pocket.[5]

In connection with our research program of using the computer-assisted molecular design (CAMD) technology to the mapping of receptor structures and to the design of suitable ligand molecules with pharmacological utility in the area of antiinfectives,[6] we have generated geometries of quinolone-type compounds by molecular mechanics calculations. We, herein, report the results of the calculated geometry, and compare them with the X-ray crystal structures in terms of accuracy and limitations.

Results and Discussions

Selection of the quinolone structures for the molecular mechanics geometry calculation is primarily based on the limited number of quinolones and their analogs whose structures are accessible through the published literature or Cam-

bridge Structure Database (CSD). Thus, we have selected the following five compounds for our study: oxolinic acid (**1a**), 5-aminooxolinic acid (**ab**), nalidixic acid(**2**), melochinone(**3**) and compound **4**. The structures were interactively constructed on the molecular modeling system and their geometries refined using the molecular mechanics algorithms incorporated into the MacroModel Molecular Modeling System.[7] In the geometry refinement based on the energy minimization procedures, we employed both the MM2 and AMBER force field parameters. It is generally known that the MM2 force field is an all-atom field and useful for a small organic molecule modeling, whereas the AMBER is a united-atom field and useful for peptides and nucleic acids.[8]

The molecular parameters obtained from the reported X-ray crystal structures and the molecular mechanics calculations are listed in Table 1 and 2 for compound 1 and 2, and 3 and 4, respectively. The individual bond length and angle of the calculated geometries generally agree with those of the crystal structures within several percentage point or degree ranges. Overall, the X-ray structures agree slightly better with the AMBER-based geometries than with the MM2-based ones, and this fact is also reflected in the superposition operation[7] of the quinolone ring moiety of the compounds examined (Table 3). The superimposition RMS's for the quinoline rings only are in the ranges of 0.026–0.053 A for the AMBER-based structures and 0.069–0.201 A for the MM2-based ones with the corresponding X-ray structures

Table 1. Molecular Parameters for Quinolones and Analogs

A. Interatomic Distances (A)

	1a			1b			2		
	X-ray	MM-2	AMBER	X-ray	MM-2	AMBER	X-ray	MM-2	AMBER
N(1)-C(2)	1.342	1.338	1.353	1.343	1.337	1.350	1.339	1.336	1.358
N(1)-C(8a)	1.400	1.348	1.361	1.392	1.348	1.361	1.398	1.336	1.361
N(1)-C(9)	1.481	1.503	1.457	1.480	1.502	1.457	1.491	1.499	1.469
C(2)-C(3)	1.368	1.337	1.406	1.361	1.337	1.404	1.362	1.339	1.406
C(3)-C(4)	1.427	1.353	1.408	1.435	1.353	1.409	1.439	1.355	1.407
C(3)-C(11)	1.483	1.482	1.490	1.489	1.481	1.492	1.480	1.483	1.490
C(4)-C(4a)	1.454	1.359	1.407	1.445	1.359	1.417	1.449	1.356	1.404
C(4)-O(14)	1.259	1.210	1.213	1.276	1.211	1.215	1.254	1.209	1.213
C(4a)-C(5)	1.417	1.403	1.412	1.436	1.403	1.423	1.409	1.470	1.399
C(4a)-C(8a)	1.405	1.405	1.420	1.432	1.405	1.425	1.390	1.340	1.411
C(5)-C(6)	1.356	1.387	1.401	1.376	1.390	1.397	1.362	1.339	1.394
C(6)-C(7)	1.384	1.374	1.379	1.361	1.374	1.376	1.393	1.465	1.400
C(6)-O(15)	1.370	1.357	1.357	1.387	1.358	1.358	—	—	—
C(7)-X(8)	1.357	1.387	1.400	1.371	1.387	1.398	1.334	1.263	1.352
C(7)-O(17)	1.365	1.357	1.357	1.373	1.357	1.357	—	—	—
C(7)-C(15)	—	—	—	—	—	—	1.498	1.504	1.510
X(8)-C(8a)	1.419	1.403	1.413	1.411	1.403	1.414	1.341	1.332	1.357
C(9)-C(10)	1.509	1.537	1.529	1.508	1.537	1.529	1.501	1.535	1.535
C(11)-O(12)	1.212	1.206	1.204	1.215	1.207	1.204	1.214	1.206	1.204
C(11)-O(13)	1.319	1.335	1.329	1.326	1.335	1.329	1.323	1.336	1.329
O(15)-C(16)	1.428	1.421	1.445	1.421	1.420	1.445	—	—	—
C(16)-O(17)	1.435	1.421	1.445	1.440	1.420	1.446	—	—	—

Table 1B. Bond Angles (deg)

	1a			1b			2		
	X-ray	MM-2	AMBER	X-ray	MM-2	AMBER	X-ray	MM-2	AMBER
C(8a)-N(1)-C(2)	120.1	119.1	119.2	120.9	119.1	119.3	119.3	118.8	118.5
C(8a)-N(1)-C(9)	121.3	123.1	122.5	121.2	123.3	122.6	120.8	120.6	119.8
C(2)-N(1)-C(9)	118.7	117.3	118.3	117.7	117.2	118.0	119.9	120.0	121.7
N(1)-C(2)-C(3)	123.6	122.1	123.3	123.4	121.6	123.3	124.4	121.7	123.7
C(2)-C(3)-C(4)	120.3	120.2	118.0	119.9	120.2	118.2	120.0	119.8	117.8
C(2)-C(3)-C(11)	117.9	119.0	119.6	118.2	119.0	118.3	118.9	119.1	119.7
C(4)-C(3)-C(11)	121.7	120.8	122.4	121.9	120.8	122.5	121.1	121.1	122.4
C(3)-C(4)-C(4a)	115.9	118.7	118.9	117.0	118.7	119.2	115.0	118.6	118.7
C(3)-C(4)-O(14)	122.7	120.4	121.6	120.8	118.9	120.1	122.9	121.7	121.8
C(4a)-C(4)-O(14)	121.4	120.9	119.5	122.1	122.3	120.7	122.1	119.9	119.5
C(4)-C(4a)-C(5)	118.5	118.8	120.0	120.7	119.6	122.2	121.7	121.1	120.4

C(4)-C(4a)-C(8a)	121.0	119.8	119.6	119.9	119.2	118.6	121.9	120.0	120.1
C(5)-C(4a)-C(8a)	120.4	121.4	120.4	119.5	121.2	119.1	116.4	118.8	119.6
C(4a)-C(5)-C(6)	117.3	117.6	118.6	115.5	117.4	119.1	119.5	117.6	119.1
C(5)-C(6)-C(7)	121.8	121.3	121.3	123.8	121.8	121.4	119.6	118.2	119.2
C(5)-C(6)-O(15)	128.4	128.6	127.7	125.3	128.4	127.3	—	—	—
C(7)-C(6)-O(15)	109.9	110.0	111.0	110.8	109.8	111.3	—	—	—
C(6)-C(7)-X(8)	123.6	121.7	121.3	123.9	121.6	121.1	122.5	121.4	121.5
C(6)-C(7)-O(17)	109.6	109.9	111.0	109.9	110.0	111.0	—	—	—
X(8)-C(7)-O(17)	126.8	128.4	127.6	126.2	128.4	127.9	—	—	—
C(6)-C(7)-C(15)	—	—	—	—	—	—	120.9	122.0	119.3
C(15)-C(7)-X(8)	—	—	—	—	—	—	116.6	116.6	119.2
C(7)-X(8)-C(8a)	116.0	118.5	118.8	115.1	118.2	119.1	117.4	122.2	120.5
X(8)-C(8a)-N(1)	119.9	122.1	119.6	119.0	121.7	118.6	116.1	117.0	118.6
X(8)-C(8a)-C(4a)	121.0	119.3	119.7	122.2	119.7	120.1	124.6	121.9	120.3
C(4a)-C(8a)-N(1)	119.1	118.6	120.8	118.7	118.6	121.3	119.3	121.1	121.1
N(1)-C(9)-C(10)	112.1	112.5	110.2	111.0	112.6	110.3	112.3	112.1	114.1
C(3)-C(11)-O(12)	123.3	124.5	127.3	123.1	124.4	127.4	123.5	124.6	127.2
C(3)-C(11)-O(13)	115.8	119.4	111.0	115.6	119.5	111.0	115.5	119.2	111.0
O(12)-C(11)-O(13)	120.9	116.0	121.7	121.3	116.2	121.6	121.0	116.3	121.9
C(6)-O(15)-C(16)	105.9	106.0	104.4	103.9	106.1	104.2	—	—	—
O(15)-C(16)-O(17)	107.8	108.0	109.1	108.4	108.0	109.2	—	—	—
C(16)-O(17)-C(7)	106.1	106.1	104.4	104.7	106.1	104.3	—	—	—

Table 2. Molecular Parameters for Quinolones and Analogs

A. Interatomic Distances (A)

	3			4	
	X-ray	MM-2	AMBER	X-ray	MM-2
N(1)-C(2)	1.350	1.340	1.367	1.38	1.333
N(1)-C(8a)	1.372	1.330	1.368	1.42	1.358
N(1)-C(13)	—	—	—	1.44	1.357
C(2)-C(3)	1.368	1.350	1.339	1.42	1.462
C(2)-X(9)	1.498	1.513	1.515	1.30	1.254
C(3)-C(4)	1.431	1.364	1.468	1.36	1.340
C(3)-X(10)	1.384	1.374	1.376	1.45	1.430
C(4)-C(4a)	1.429	1.358	1.472	1.43	1.499
C(4)-X(12)	1.256	1.213	1.231	1.51	1.490
C(4a)-C(5)	1.426	1.405	1.425	1.43	1.398
C(4a)-C(8a)	—	1.389	1.346	1.42	1.403
C(5)-C(6)	1.398	1.401	1.414	1.41	1.392
C(5)-C(13)	1.514	1.512	1.511	—	—
C(6)-C(7)	1.411	1.389	1.403	1.40	1.391
C(6)-C(17)	1.492	1.504	1.516	—	—
C(7)-C(8)	1.360	1.392	1.399	1.43	1.393
C(8)-C(8a)	1.407	1.392	1.404	1.40	1.401
X(10)-Y(11)	1.429	1.402	1.431	1.15	1.163
C(13)-O(14)	—	—	—	1.20	1.259
C(13)-N(15)	—	—	—	1.39	1.350
N(15)-C(16)	—	—	—	1.41	1.341
C(16)-O(17)	—	—	—	1.20	1.255
C(16)-N(9)	—	—	—	1.37	1.334
O(18)-C(12)	—	—	—	1.21	1.209
O(19)-C(12)	—	—	—	1.32	1.349
O(19)-C(20)	—	—	—	1.49	1.407

Table 2B. Bond Angles (deg)

	3			4	
	X-ray	MM-2	AMBER	X-ray	MM-2
C(8a)-N(1)-C(2)	122.8	122.8	120.5	122.7	118.6
C(8a)-N(1)-C(13)	—	—	—	120.2	125.9
C(13)-N(1)-C(2)	—	—	—	117.0	115.4
N(1)-C(2)-C(3)	119.3	118.9	121.9	117.3	122.6
N(1)-C(2)-X(9)	117.1	115.2	117.5	125.2	123.1
X(9)-C(2)-C(3)	123.5	125.8	120.7	117.5	114.2
C(2)-C(3)-C(4)	122.9	118.8	120.1	122.1	119.8
C(2)-C(3)-X(10)	118.8	130.4	118.9	117.5	116.7
X(10-C(3)-C(4)	118.3	110.8	120.9	120.4	123.5
C(3)-C(4)-C(4a)	116.3	120.7	115.7	119.9	117.2
C(3)-C(4)-X(12)	120.7	119.2	120.9	118.7	120.9
X(12)-C(4)-C(4a)	123.0	120.1	123.4	121.2	121.8
C(4)-C(4a)-C(5)	123.8	122.9	121.6	120.7	121.5
C(4)-C(4a)-C(8a)	119.6	116.9	118.9	120.1	118.3
C(8a)-C(4a)-C(5)	118.5	120.1	119.5	119.2	120.1
C(4a)-C(5)-C(6)	119.6	118.5	119.9	119.8	120.7
C(5)-C(6)-C(7)	119.6	119.6	118.5	119.9	119.0
C(6)-C(7)-C(8)	121.8	121.1	119.7	121.5	119.5
C(7)-C(8)-C(8a)	119.4	119.7	120.4	118.2	121.6
C(3)-X(10)-Y(11)	112.8	123.2	116.6	178.7	178.3
N(1)-C(13)-N(15)	—	—	—	114.0	122.2
C(13)-N(15)-C(16)	—	—	—	123.7	117.1
N(15)-C(16)-N(9)	—	—	—	117.0	119.4
C(2)-N(9)-C(16)	—	—	—	119.1	121.9

Table 3. The Overall Superimposition of the Quinoline Rings*

Compound	X-ray and MM2	X-ray and AMBER
1a	0.069	0.026
1b	0.103	0.027
2	0.080	0.032
3	0.175	0.055
4	0.201	—

*Superimposition root mean square (RMS) expressed in angstram unit.

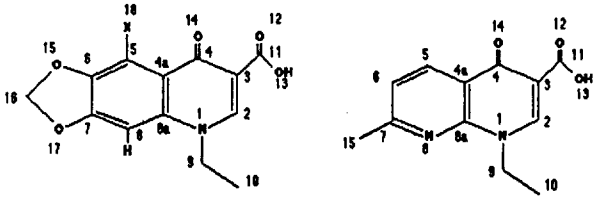

1a. X = H
b. X = NH_2

2

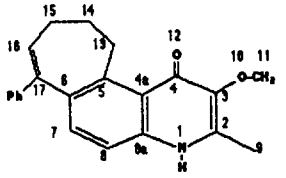

3

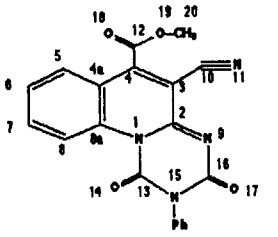

4

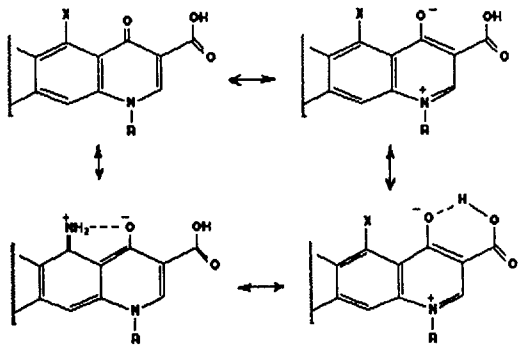

Scheme 1. (X = H or NH_2)

as references.

The comparison of the X-ray crystal geometry of quinolones with the calculated structures shows several instructive features. First, the X-ray structures all show essentially planar bicyclic ring geometry, although in nalidixic acid both rings possess some degrees of deviations from planarity. The calculated structures, both MM2 and AMBER, also display the virtually planar bicyclic rings. Second, there exists a considerable double bond localization in the pyridone ring as well as the benzene ring moieties in the crystal structures. For example, the two C-N bonds in the pyridone ring differ by as much as 0.059 A in nalidixic acid(**2**). But the force field calculations are incapable of reproducing the double bond localization to the similar extent. Third, the C=O bond length in the X-ray geometry of the quinolone ring is interpreted to reflect the degree of contributions from the dipolar structure and the possible hydrogen bonding of the β-keto acid residue (Scheme 1). The C°O bond lengths were found to be in the range of 1.254–1.259 A in oxolinic acid, nalidixic acid and melochinone. However, the C=O bond length (1.276 A) found in 5-aminioxolinic acid (**1b**) is appreciably longer than that of oxolinic acid, presumably due to the contribution of an additonal dipolar structure involving the 5-amino group. The C=O bond length elongation expected from such resonance contributions and hydrogen bonding is not observed in the calculated geometries.

Table 4. Interatomic Distances of O(13)/O(12) from O(14). (A)

Compound	X-ray	MM2	AMBER
1a	2.545/4.106	2.676/3.824	4.145/2.777
1b	2.518/4.094	2.672/3.796	4.122/2.752
2	2.529/4.105	2.670/3.870	4.148/2.780

Table 5. Torsional Angle C(2)-C(9)-C(10)*

Compound	X-ray	MM2	AMBER
1a	−102.3°	±87.5°	−87.9° and +92.1°
1b	−97.5°	±87.2°	−87.9° and +92.1°
2	−99.0°	±88.7°	−91.5° and +88.5°

*The torsional angle in the lowest energy conformation after plotting the steric map.

Fourth, a strong hydrogen bonding between the O(14) atom and the carboxylic acid residue has been strongly suggested by the X-ray crystal data of quinolone carboxylic acid **1** and **2**. For instance, the interatomic distances between the O(14) atom and the O(13) atom, 2.518 A for 5-aminooxolinic acid(**1b**) to 2.545 A for oxolinic acid(**1a**), are quite appropriate for hydrogen bonding. We have examined the total steric energies of compounds **1** and **2** with varying degrees of torsional angle C(4)-C(3)-C(11)-O(13). The interatomic distances of O(13) and O(12) from the carbonyl oxygen in the lowest energy conformations are listed in Table 4 together with the corresponding distances found in the X-ray crystal structures. From the data, it may be noted that the MM2 calculations are capable of placing the hydroxyl part of the carboxylate structure in such a way that some degree of hydrogen bonding is possible between the O(14) and O(13) atoms, whereas AMBER calculations do not clearly distinguish the hydroxyl part from the carbonyl part of the carboxylate functionality. Fifth, the N(1) ethyl substitutent in oxolinic acid, 5-aminooxolinic acid and nalidixic acid is nearly perpendiculat to the ring plane. The C(2)-N(1)-C(9)-C(10) torsional angles in these compounds are −102.3°, −97.5°, and −99.0°, respectively. We have also calculated the total steric energies of N(1) ethyl quinolones with varying degree of torsional angle C(2)-N(1)-C(9)-C(10). The torsional angles in the lowest energy conformations are shown in Table 5. The calculated tortional angles are found to be in reasonable agreements with those of the X-ray crystal structures, in spite of the fact that torsional angles are often distorted by the crystal packing effects.[8a]

In conclusion, it was found that despite the apparent shortcomings associated with calculating electronic contributions by resonance and hydrogen bonding, the combined

moleculr mechanics methods were capable of reproducing the overall ring geometry and the torsional angle dispositions of N(1)-ethyl and 3-carboxylate substituents of the quinolone antibacterials. The torsional problem of 7-amino substituents such as piperazines and pyrrolidines on the quinolone, and molecular modeling studies of quinolone antibacterials in view of the recently proposed cooperative quinolone-DNA binding model for the gyrase inhibition are currently in progress.

Experimental Methods

The molecular modeling system at POSTECH consists of Evans & Sutherland PS 390 graphics station linked to VAX 8800 running the MacroModel Molecular Modeling software (v. 2.5). The MacroModel implementation of MM2 and AMBER differs from the standard versions in several ways and they were previously described.[6,7]

The energy minimizations were carried out to the preset convergence criterion (RMS energy gradient less than 0.05 KJoule/A) initially by the Steepest Descent(SD) method followed by block diagonal Newton-Raphson(BDNR) method. For the given structure, molecular hydrogens were added in the Organic Input Mode before the MM2 calculations. Since the AMBER method requires hydrogens only at the heteroatoms, other types of hydrogens were deleted from the MM2 minimized structures before the AMBER calculations. The torsional angle optimizations were performed by drawing the steric energy maps for both 1 and 2 angle search methods in the Map Energy Submode. The angle searches were done by using Energy Calculation rather than Approxiate Energy Calculation, and the angle resolution was 10 degree in global. The X-ray crystal molecular parameters were taken from CSD sources[9] as well as literature for compounds 1-4.[10]

Acknowledgement. We wish to thank professor W. Clark Still of Columbia University for loaning the MacroModel Molecular Modeling Program. The financial support from Korea Science and Engineering Foundation is gratefully acknowledged.

References

1. (a) R. Albrecht, *Prog. Drug Res.*, **21**, 9 (1977); (b) G. C. Crumplin, J. M. Midgley anf J. T. Smith, in "Topics in Antibiotic Chemistry", Ed. P. G. Sammes, Vol. 3, John Wiley, New York 1980; (c) H. J. Zeiler, in "Trends in Medicinal Chemistry", Ed. E. Mutscheler and E. Winterfeldt, VCH, Weinheim, 1987.
2. L. L. Shen and A. G. Pernet, *Proc. Nat. Acad. Sci., USA*, **82**, 307 (1985).
3. K. Timmers and R. Strenglenz, *Bioinorg. Chem.*, **9**, 145 (1978).
4. S. K. Chung, J. H. Sun, and Y. J. Oh, unpublished results, 1990.
5. L. L. Shen, L. A. Mitscher, P. N. Sharma, T. J. O'Donnell, D. W. T. Chu, C. S. Cooper, T. Rosen and A. G. Pernet, *Biochem.*, **28**, 3886 (1989).
6. (a) S. K. Chung and D. F. Chodosh, *Bull. Kor. Chem. Soc.*, **10**, 185 (1989); (b) S. K. Chung, *ibid.*, **10**, 216 (1989).
7. W. C. Still, Columbia University, MacroModel Molecular Modeling System, v. 2. 5., March 1989.
8. Molecular Mechanics", U. Berkert and N. L. Allinger, *Amr. Chem. Soc.*, Washington, D. C. 1982; (b) N. L. Allinger, *J. Am. Chem. Soc.*, **99**, 8127 (1977); (c) S. J. Weiner, P. A. Kollman, D. Case, U.C. Singh, G. Alagona, S. Profeta, and P. Weiner, *ibid.*, **106**, 764 (1984).
9. (a) Cambridge Structureal Database, v. 3.4, January 1989, Cambridge Crystallographic Data Center, University Chemistry Laboratory, Cambridge; (b) F. H. Allen, O. Kennard and R. Taylor, *Acc. Chem. Res.*, **16**, 146 (1983).
10. (a) M. Cygler and C. P. Huber, *Acta Cryst.*, **C41**, 1052 (1985); (b) M. Czygler, G. Argay, J. Frank, Z. Meszaros, L. Kutschabsky and G. Reck, *ibid.*, **B32**, 3124 (1976); (c) C. P. Huber, D. S. S. Gowda and K. R. Acharya, *ibid.*, **B36**, 497 (1980); (d) G. J. Kapadia, B. D. Paul, J. V. Silverton, H. M. Fales and E. A. Sokoloski, *J. Am. Chem. Soc.*, **97**, 6814 (1975); (e) E. Wilhelm and R. Hoge, *Cryst. Struct. Comm.*, **5**, 13 (1976).